2015

Quantifying Vitamin K-dependent Holoprotein Compaction caused by differential γ-carboxylation using HPSEC

Nicholas C. Vanderslice
University of Nebraska-Lincoln, vanderslice.nicholas@gmail.com

Amanda S. Messer
University of Nebraska-Lincoln, asmesser3@gmail.com

Kanagasabai Vadivel
University of California, Los Angeles, kvadivel@mednet.ucla.edu

S. Paul Bajaj
University of California, Los Angeles, pbajaj@mednet.ucla.edu

Martin Phillips
University of California, Los Angeles, mlphill@ucla.edu

See next page for additional authors

HHS Public Access

Author manuscript

Anal Biochem. Author manuscript; available in PMC 2016 June 15.

Published in final edited form as:

Anal Biochem. 2015 June 15; 479: 6–14. doi:10.1016/j.ab.2015.03.019.

Quantifying Vitamin K-dependent Holoprotein Compaction caused by differential γ-carboxylation using HPSEC

Nicholas C. Vanderslice[a], **Amanda S. Messer**[a,b], **Kanagasabai Vadivel**[b], **S. Paul Bajaj**[b], **Martin Phillips**[c], **Mostafa Fatemi**[a], **Weijie Xu**[a], and **William H. Velander**[a,*]

[a]Protein Purification and Characterization Laboratories, Department of Chemical and Biomolecular Engineering, 207 Othmer Hall, University of Nebraska, Lincoln 68588, USA

[b]Protein Science Laboratory, UCLA/Orthopaedic Hospital, Department of Orthopaedic Surgery and Molecular Biology Institute, 615 Charles E. Young Dr South, University of California, Los Angeles 90095, USA

[c]UCLA-DOE Biochemistry Instrumentation Facility, Department of Chemistry and Biochemistry, 607 Charles E. Young Drive East, UCLA, Los Angeles, CA 90095, USA

Abstract

This study uses high-pressure size exclusion chromatography (HPSEC) to quantify divalent metal ion (X^{2+})-induced compaction found in vitamin K dependent (VKD) proteins. Multiple X^{2+} binding sites formed by the presence of up to 12 -carboxyglutamic acid residues (Gla) are present in plasma-derived (pd-) and recombinant (r-) Factor IX (FIX). Analytical ultracentrifugation (AUC) was used to calibrate the Stokes radius (R) measured by HPSEC. A compaction of pd-FIX caused by the filling of Ca^{2+} and Mg^{2+} binding sites resulting in a 5-6% decrease in radius of hydration as observed by HPSEC. The filling of Ca^{2+} sites resulted greater compaction than for Mg^{2+} alone where this effect was additive or greater when both ions were present at physiologic levels. Less X^{2+} induced compaction was observed in r-FIX with lower Gla content populations which enabled the separation of biologically active from inactive r-FIX species by HPSEC. HPSEC was sensitive to R changes of ~0.01 nm that enabled the detection of FIX compaction that was likely cooperative in nature between lower avidity X^{2+} sites of the Gla domain and higher X^{2+} avidity sites of the EGF1-like domain.

*Corresponding Author. William H Velander, 207 Othmer Hall, 820 N. 16th St., University of Nebraska-Lincoln, Lincoln, NE 68588-0668; Tel: 402-472-3697, Fax: 402-472-6989; wvelander2@unl.edu.
Nicholas Vanderslice, vanderslice.nicholas@gmail.com
Amanda S. Messer, asmesser3@gmail.com
Kanagasabai Vadivel, kvadivel@mednet.ucla.edu
S. Paul Bajaj, pbajaj@mednet.ucla.edu
Martin Phillips, mlphill@ucla.edu
Mostafa Fatemi, mfatemi2@unl.edu
Weijie Xu, weijiexuchn@gmail.com

Keywords

High Pressure Size Exclusion Chromatography; Vitamin K Dependent protein; γ-carboxylation; Factor IX

1. Introduction

The Vitamin K-dependent (VKD) family of plasma proteins are key participants in the coagulation cascade of hemostasis[1,2]. This family includes the anticoagulant proteins C, S and Z, and the procoagulant factors (F) VII, IX, X and prothrombin [3]. The first nine amino terminal glutamic acids of these glycoproteins are well conserved and are -carboxylated to form "γ-carboxyglutamic acid (Gla) residues". These residues are part of the "Gla domain" which contains 7-8 divalent metal (X^{2+}) binding sites that are essential to the function of VKD coagulation proteins. This function is highly regulated by the formation of multi-protein complexes at the phospholipid surfaces of injured vascular endothelium. A spatially quantitative measure of overall holoprotein folding as a function X^{2+} site filling would provide insight into the process by which coagulation protein complexes are formed.

The conformational attributes of the Gla domain have been well studied using NMR and x-ray crystallography [4-9]. Since VKD proteins are also glycoproteins the Gla domain is usually isolated to enable study by crystallography. The Gla domain has also been studied using X^{2+}, conformational-dependent monoclonal antibodies [10-14]. These previous studies have observed the cooperative folding within the Gla domain that occurs with filling of Ca^{2+}- and Mg^{2+}-binding sites [4,5,8,15]. Conformational changes have been also observed in all the VKD coagulation proteins using fluorescence quenching due to specific X^{2+} site binding [8,16,17]. FIX is an example of a VKD protein with X^{2+} binding sites not only in the Gla domain but it also contains two additional Gla residues that help to form an additional Mg^{2+} site [18-20]. FIX also contains a Ca^{2+} site in one of two epidermal growth factor-like domains and also in its C-terminal serine protease domain [1,2].

Recombinant biosynthesis of VKD proteins frequently results in subpopulations of partially carboxylated proteins with modified structure and function [19,21-24]. As with other VKD proteins, recombinant (r-) FIX has important uses as a biotherapeutic where partially and fully -carboxylated structures yield different biological activity [19,24]. The high-pressure size exclusion chromatography (HPSEC) method presented here provides a quantitative assessment of overall changes in VKD macromolecular extension due to filling of the Ca^{2+} and Mg^{2+} sites that can be directly correlated with *in vitro* coagulation activity. This technique is demonstrated using plasma-derived (pd-) FIX with a full complement of 10 total X^{2+} binding sites that is compared to r-FIX populations with less γ-carboxylation.

2. Experimental

2.1. Reagents

All buffer components were purchased from VWR International LLC (Radnor, PA, USA) or Thermo Fisher Scientific (Waltham, MA, USA) or Sigma (St. Louis, MO, USA) unless otherwise stated. In order to minimize degradation, purification processes were performed at

4°C. The stocks of pd, immunoaffinity purified, therapeutic grade FIX (Mononine, CSL Behring, USA) were expired for clinical use, but when used in experiments, exhibited full procoagulant activity (150-250 U/mg). Human FIX from the milk of transgenic swine (r-FIX) was purified using a modified version of the procedure of Lindsay et al. [25]. HPSEC was used to isolate the purified sample into low carboxylated zymogen r-FIX that was inactive (<10 U/mg), zymogen r-FIX that had native coagulation activity (150-200 U/mg), and activated r-FIX (r-FIXa) (>3000 U/mg). Inactive and active r-FIX contained no r-FIXa according to SDS-PAGE. All activities were confirmed by one-stage clotting assay [25-27].

2.2. High-Pressure Size Exclusion Chromatography

The FIX products were concentrated and exchanged into 20 mM Tris, 200 mM NaCl, pH 7.0 (running buffer) using an Amicon Ultra 10 kDa molecular cut off centrifugal filter (Millipore, Billerica, MA, USA). The running buffers were treated with the sodium form of Chelex Analytical Grade 100 resin (Bio-Rad Laboratories, Hercules, CA USA) to remove X^{2+} contamination. Some studies used running buffer that contained $CaCl_2$ and or $MgCl_2$ which was added after Chelex 100 resin treatment. All injected samples were formulated with Chelex treated buffer. All sample injection volumes were less than 50 μL, and were diluted by a factor of at least 10-fold by the 500 μL buffer volume in the sample loop. The FIX products were loaded onto a 60 cm X 2.15 cm I.D. TSK gel G3000SW column (Tosoh Bioscience, King of Prussia, PA, USA) equipped with a guard column and a pre-filter.

Briefly, the chromatography was performed on the Knauer (Berlin, Germany) Smartline chromatography station described above. Flow rate was set at a constant 0.5 mL/min and the run length was 45 minutes for all studies. Effluent's absorbance was measured at an absorbance of 280 nm. Samples were run in triplicates and the center of the elution peaks were used to calculate residence time (with standard deviation <0.016). All elution volumes can be found by multiplying the elution time by 0.5 mL/min.

2.3. Sodium Dodecylsulfate-Polyacrylamide Gel Electrophoresis (SDS-PAGE)

Samples were analyzed by SDS-PAGE stained with colloidal Blue gel stain (Invitrogen, Carlsbad, CA, USA) using Invitrogen Novex precast gels and the Invitrogen Surelock XL apparatus. All gels were NuPage 12% Bis-Tris run with 2-(N-morpholino) ethanesulfonic acid (MES) running buffer (Invitrogen). Briefly, samples were mixed with 4x LDS sample buffer (Invitrogen) and deionized water followed by heating at 75 °C for 10 min. For reduced gels, samples were mixed with 10x reducing agent (Invitrogen) prior to heating.

2.4. Analytical Ultracentrifuge

pd-FIX in 0.15 M NaCl, 50 mM Tris, pH 7.5 with either 10mM EDTA or $CaCl_2$ and/or $MgCl_2$ was examined by sedimentation velocity in a Beckman Optima XL-A analytical ultracentrifuge at 52,000 or 55,000 rpm and 20 °C in 12 mm path length double sector cells using absorption optics at 280 nm. All samples were at the same protein concentration, 0.3 mg/ml. Apparent sedimentation coefficient distributions, uncorrected for diffusion, were determined as g(s) plots using the Beckman Origin based software (Version 3.01). These plots display a function proportional to the weight fraction of material with a given sedimentation coefficient, s. The function g(s) was calculated as:

$$g(s) = (dc/dt)(1/c_o)\left(\omega^2 t^2/ln(r_m/r)\right)\left(r^2/{r_m}^2\right);$$

where s is the sedimentation coefficient, ω is the angular velocity of the rotor, c_o is the initial concentration, r is the radius, r_m is the radius of the meniscus, and t is time. The x-axis is converted to sedimentation coefficient by:

$$s = \left(1/\omega^2 t\right)(ln(r/r_m))$$

These plots display a function proportional to the weight fraction of material with a given sedimentation coefficient, s [28]. The $S_{20,w}$ values were calculated using a partial specific volume which was corrected to a value of 0.708 as determined by the amino acid and carbohydrate composition of FIX [29,30]. The Stokes radius (R) was calculated using a molecular weight of 62,800. R is inversely proportional to the sedimentation coefficient, $S_{20,w}$, where compaction of the pd-FIX increases the sedimentation coefficient. Specifically, the sedimentation coefficient was used to calculate R defined by the relationship:

$$s = [(M)(1-\tilde{v})(\rho)] / [(N)(6\pi)(\eta)(R)]$$

where M is the molecular weight, $\tilde{V}$ is the partial specific volume, ρ is the solvent density, N is Avogadro's Number and η is the viscosity [31].

2.5. Modeling of X^{2+} Free and Bound pd-FIX

The X^{2+} equilibrated solution structures of pd-FIX were obtained from Perera [32]. The MODELLER program [33] was employed to model the X^{2+} free pd-FIX holoprotein by additionally utilizing NMR structures reported for pd-FIX Gla domain (PDB ID: 1CFX, [8]) as templates. No molecular shape was apriori assumed as part of the model. The built models were further refined by energy minimization using the CHARMM program with CHARMM19 force field [34] consisting of 50 steps of Steepest Descent, followed by 500 steps of Adopted Basis Newton-Raphson. Harmonic restraints of 10 kcal/mol/$Å^2$ were applied on the C^α atoms of the protein during the entire minimization.

2.6. Mass Spectrometry of the Gla Domain

The γ-carboxylation of the Gla domain of pd-FIX and r-FIX were assessed using LC-ESI-TOF mass spectrometry (MS). Samples of r-FIX and active r-FIX were activated with Factor XIa (FXIa) (Haemtech, Essex Junction, VT) using a 1:100 (w:w) enzyme to substrate ratio in 5mM $CaCl_2$, 1X TBS, pH 7.4 at 37°C for 1.0 hour. After activation, the samples were quenched with 1.2 moles of EDTA per mole of calcium and stored at -80°C until further analysis.

MS analysis was performed on an Agilent 1200 capLC system with an Agilent 6210 ESI-TOF MS [35]. Solvent A was 0.1% formic acid (Fluka) (v/v) in deionized water. Solvent B was 0.1% formic acid (v/v) in acetonitrile (Burdick and Jackson). The column was an

Agilent 300SB-C8 Poroshell column: 7.5 cm L x 0.5 mm ID, 5 micron particle size. MS data were acquired with MassHunter in positive mode with the following parameters: 4000 V source voltage, 325°C nebulizing gas temperature, 7 L/min gas flow rate, internal reference mass of 922.01 m/z. MS data were analyzed using Agilent's Qualitative Analysis (version B.01.03).

2.7 One stage coagulation assay

FIX specific activity was determined using a one stage coagulation assay [36]. Briefly, 50 μL each of PTT Automate 5 reagent (Diagnostica Stago, Inc., Parsippany, NJ, USA), 50 μL of FIX deficient plasma (George King Bio-Medical, Overland Park, Kansas, USA), or 50 μL sample was added to the measurement cuvette and incubated at 37 °C for 3 min. After the incubation period, 50 μL of 25 mM $CaCl_2$ was added and the clotting time was measured using the STart Hemostasis Analyzer (Diagnostica Stago, Inc., Parsippany, NJ). Normal human plasma (Diagnostica Stago, Inc., Parsippany, NJ) was used as the defined standard reference where normal human plasma contains 1 international unit of FIX clotting activity per mL. The concentration of purified r-FIX was determined spectrophotometrically at 280 nm using an extinction coefficient, $\varepsilon^{1\%}$ =13.4.

3. Results and discussion

3.1. Predicted holoprotein size changes in pd-FIX induced by X^{2+}

Herein, we use HPSEC calibrated by AUC to quantitatively measure holoprotein folding contributed by different domains due to the filling of both Ca^{2+}/Mg^{2+} sites relative to Ca^{2+} and Mg^{2+}sites alone. Molecular modeling of X-ray crystallography and NMR data was used to help predict the nature and magnitude of the holoprotein size change that would be expected from the filling of all X^{2+} sites within different domains of FIX. The predicted structures of X^{2+} free and bound of FIX containing the full complement of 12 Gla residues are shown in Fig. 1. In the presence of physiologic levels of Ca^{2+} (~1.1 mM) and Mg^{2+} (~0.6 mM), four sites (numbered 2, 3, 5 and 6) are occupied by Ca^{2+} and three (numbered 1, 4, and 7) by Mg^{2+} [4,37]. It is important to note that all metal sites in the Gla domain will be filled by Ca^{2+} at greater than 2 mM in the absence of Mg^{2+}. The Mg^{2+}-site 4 is predicted to switch to Ca^{2+} upon binding of the Gla domain to phospholipid (PL) [38].

Our modeling predicted a linear structure with a more extended structure in the case of vacant relative to X^{2+} filled sites. Our model predicted an overall radius of gyration (Rg) of 34.46 Å for the X^{2+} free state and 32.75 Å for the X^{2+} filled pd-FIX holoprotein with a relative change in Rg of ~5%. As expected, the largest contributor to changes in molecular extension arose from the filling of both Ca^{2+} and Mg^{2+} sites in the core Gla domain (Fig. 1A, 1B). Currently, there is a lack of crystallographic data that studies the Gla domain under conditions having only Mg^{2+} filled sites.

Interestingly, other more subtle changes with X^{2+} dependent conformation were predicted by our model which were caused by domains outside of core Gla domain. For example, the Gla residues at amino acid 36 and 40 do not affect FIX biological activity *in vitro* [19] and are not present in other VKD proteins. Recombinant biosynthesis frequently results in the lack of γ-carboxylation at these two positions and therefore the inability to form the number

eight X^{2+} site that is Mg^{2+}-specific [7,19]. Our model also predicts that the Ca^{2+} specific binding site which occurs in the EGF1-like domain [39] will be the next largest contribution to the overall compaction of pd-FIX relative to the Gla domain. The Ca^{2+} specific site in the protease domain [40,41] was predicted to give a negligible contribution to pd-FIX compaction.

3.2. Homogeneity of the pd-FIX and rFIX preparations studied here

Previous studies have reported protein aggregation in pd-FIX in the presence of X^{2+} observed by AUC at concentrations of >0.3 mg pd-FIX/ml [16]. Thus, we used SDS-PAGE and HPSEC to ascertain the extent of aggregation in the pd-FIX and r-FIX preparations studied here. For example, Fig. 2A shows SDS-PAGE analysis under non-reducing conditions of immunoaffinity purified, therapeutic grade pd-FIX where an estimated 100 ng band at 47 kDa was observed. This subpopulation of proteolyzed FIX is commonly present in pd-FIX and has a 10 kDa fragment removed from its carboxy- terminus [42]. Thus, we estimate that the pd-FIX here contained >95% zymogen having a Mr of 57 kDa and 0.1-5% proteolyzed pd-FIX. Fig. 2B and 2C show the typical HPSEC chromatographic profiles for injections of 25 and 50 μg pd-FIX that was obtained at physiologic pH in the presence of 1.1 mM Ca^{2+} alone and of 0.6 mM Mg^{2+} alone, respectively. Fig. 3-5 present the HPSEC chromatographic behavior for analysis of 100 μg injections. In all cases studied, the HPSEC behavior possessed a single predominant and symmetrical peak. In the case of the 100 μg injection, a peak height signal was observed which was about 4- and 2-fold larger than those observed for the 25 μg and 50 μg injections. Taken together, the samples predominately contained intact pd-FIX which showed no appreciable tendency to form aggregates at any of the X^{2+} and protein concentrations examined here by HPSEC or AUC.

3.3. HPSEC Elution Profile Sensitivity to pd-FIX size changes resulting from presence of Ca^{2+} alone

We observed changes in overall HPSEC elution times of FIX in sequence of chromatographies with incrementally higher Ca^{2+} levels known to metal site filling in the higher avidity catalytic and EGF1-like domains followed by the lower avidity Gla domain. For example, Fig. 3A shows the HPSEC chromatographic profiles for pd-FIX collected over a range of sub- to supra-physiologic Ca^{2+} levels in the absence of Mg^{2+}. A baseline residence time of about 17.1 minutes was obtained for the elution peak of pd-FIX when chromatographed under X^{2+} free conditions (Fig. 3A: curve 1). When chromatographed at a subphysiologic level of 0.5 mM Ca^{2+} at which higher avidity sites in the catalytic and EGF-1 like domains should approach being filled [39, 43] the residence time shifted to a longer time of 17.9 minutes (Fig. 3A: curve 2). This compaction phenomena was observed to increase with increasing levels of Ca^{2+} (Figure 3A: curve 3-5) up to a supra-physiologic concentration of 10 mM Ca^{2+} where a 19.0 elution peak residence time was observed. An asymptotic level of lengthening residence times of about 19.05 minutes occurred when pd-FIX was chromatographed at 15 mM Ca^{2+} (Fig. 3A: curve 6). At this supra-physiologic conditions, each X^{2+} binding site in the core Gla domain has been previously reported to be occupied by Ca^{2+} [38].

Using a plot of HPSEC elution peak residence times versus Ca^{2+}concentration, the change in chromatographic behavior seen at different X^{2+} ion concentrations can be correlated with the filling of specific sites as measured by other techniques [7,19,39-41,43,44]. Two compaction regimes were observed by HPSEC. The inset plot of Fig. 3B shows the presence of a compaction regime occurring at a Ca^{2+} level of 0-0.5 mM. Our modeling (Figure 1) predicted that significant compaction would result from filling of the Ca^{2+} specific site in EGF1-like domain while a negligible amount of compaction would result from filling of the Ca^{2+} site in the catalytic domain. This HPSEC data is a first time direct observation of FIX holoprotein compaction as a result of the higher affinity Ca^{2+} sites filling in those domains. In contrast, a separate compaction regime that was detected at about 0.3 to 5 mM Ca^{2+} was consistent with compaction predicted for the core Gla sites. In summary, the compaction behavior of pd-FIX observed at supra-physiologic levels of Ca^{2+} is likely the combined filling of both high avidity Ca^{2+}-specific sites in the EGF1-like and protease domains along with the lower avidity Ca^{2+} sites of the Gla domain.

3.4. HPSEC Elution Profile Sensitivity to pd-FIX size changes resulting from presence of Mg^{2+} alone

We also observed changes in overall HPSEC elution times of FIX in sequence of chromatographies with incrementally higher Mg^{2+} levels known to fill the 3 sites within and the single site proximal to the core Gla domain. Starkly less compaction was observed in the presence of Mg^{2+} alone than that seen for Ca^{2+} alone (Fig. 4A). For example, the presence of the physiologic level of 0.6 mM Mg^{2+} resulted in a decreased, but discernable 0.3 minute increase in residence time shift over that of X^{2+} free buffer (Fig. 4A: curves 1 and 2). Similarly small shifts were observed at the supraphysiologic Mg^{2+} concentrations of 5 and 10 with no shift detectable at 15 mM Mg^{2+} (Fig. 4A: curves 3, 4, and 5 respectively).

A single compaction regime was observed in a plot of the net residence time shift versus Mg^{2+} concentration over the range of sub to supra-physiologic levels of Mg^{2+} (Fig. 4B). Past studies have shown that all Mg^{2+}-specific sites within the core Gla domain of VKD coagulation proteins are at least half-maximally filled at physiologic levels of Mg^{2+} [45]. The compaction response observed by HPSEC seen with Mg^{2+} relative to Ca^{2+} is consistent with the lesser number of Mg^{2+} sites and their peripheral positioning in the Gla domain (Fig. 1B).

3.5. HPSEC elution profile sensitivity to pd-FIX compaction resulting from presence of both Mg^{2+} and Ca^{2+}

We investigated the dependence of the compacted conformation on the simultaneous presence of both X^{2+}. In the presence of physiologic levels of both Mg^{2+} and Ca^{2+} (Fig. 5: Curve 4), pd-FIX eluted at later times than that obtained in the presence of no X^{2+} (Fig. 5: curve 1), 0.6 mM Mg^{2+} alone (Fig. 5: curve 2) and 1.1 mM Ca^{2+} alone (Fig. 5: curve 3). Importantly, the HPSEC residence time shift resulting from the simultaneous presence of both X^{2+} was essentially additive relative to that obtained in the presence of Ca^{2+} and Mg^{2+} alone. This is indicative of the respective X^{2+} specificity of sites which contribute to pd-FIX compaction.

It is noted that the compaction of pd-FIX resulting from the filling of the both Ca^{2+} and Mg^{2+} metal binding sites within the Gla domain can be visualized by the organization and formation of the -loop (Fig. 1B). The -loop has been shown to be an important structure necessary for biological activity [7,37,38,46]. X^{2+} sites 2 to 6 strongly affect the positioning of the -loop which spans amino acids 1-14 and is central to phospholipid binding. Upon binding of phospholipid, site 4 is converted from a Mg^{2+} to a Ca^{2+} site which results in profound repositioning of the -loop to the interior of the Gla domain [7,38]. Supra-physiologic concentrations of Ca^{2+} can also result in the filling of site 4 by Ca^{2+} and a repositioning of the -loop. In the absence of Mg^{2+}, all sites are occupied by Ca^{2+} at 2 mM [38] while at physiologic levels of Ca^{2+} and Mg^{2+} positions 1, 4, 7 and 8 are occupied by Mg^{2+}. However, at supraphysiologic levels at which asymptotic compaction by Ca^{2+} was observed here by HPSEC, Mg^{2+} at site 4 would be displaced by Ca^{2+} [38].

3.6. HPSEC observed changes in compaction for partially carboxylated r-FIX

We investigated the X^{2+} dependent compaction properties of r-FIX having different extents of γ-carboxylation and coagulation activity. We observed a difference in the compaction between high and low Gla content r-FIX at 10 mM Ca^{2+}(Fig. 6). Table 1 presents a comparison of biotherapeutic grade pd-FIX with the two major HPSEC chromatographic fractions obtained from a pool of already highly purified r-FIX. Peak 1 possessed the shortest elution time and it consisted of lower Gla content r-FIX that was inactive. Peak 2 eluted at a longer time and possessed a specific coagulation activity that was comparable to therapeutic grade pd-FIX. It also predominately consisted of 10-12 -carboxylated Gla species Gla content r-FIX. The extent of γ-carboxylation in r-FIX has been previously shown to be a primary determinant of coagulation activity [47,48]. In summary, the inactive and active r-FIX fractions demonstrated starkly different Ca^{2+} dependent compaction (Fig. 7 A and B).

We observed similar X^{2+} dependent compaction regimes for the active r-FIX fraction as that observed in pd-FIX. In contrast, the inactive r-FIX fraction exhibited a general lack of compaction. Interestingly, at the level of <0.4 mM Ca^{2+}, the inactive r-FIX fraction displayed minimal compaction while both the active r-FIX and pd-FIX displayed a similar but distinguishable compaction. This suggests that the compaction induced by the high affinity Ca^{2+} site in the EGF1-like domain which is proximal to the Gla domain is affected by Gla domain folding. At >0.4 mM Ca^{2+}, the asymptotic maximum in the total residence time shift was reduced by 82% for inactive r-FIX relative to active r-FIX fractions.

For chromatographies done in the presence of Mg^{2+} alone, the compaction of the active r-FIX fraction was nearly identical to that of fully -carboxylated pd-FIX. In contrast, the inactive r-FIX fraction displayed only a <0.05 minute shift in compaction at 0.6-1.1 mM Mg^{2+} (Fig. 7 C and D). Thus, this lack of compaction observed using HPSEC indicates that γ-carboxylation deficiencies likely occurred at positions essential to the formation both Ca^{2+} and Mg^{2+} sites within the core Gla domain.

3.7. Analytical ultracentrifuge calibration of HPSEC for predicting R

We used AUC to both confirm the general compaction phenomena and to calibrate the observed HPSEC chromatographic behavior for the correlative estimation [49-51] of the Stokes hydrodynamic radius (R) at the X^{2+} ion concentrations studied here. It is important to note that past AUC studies of VKD coagulation proteins were used to examine for the presence or absence of aggregation. Table 2 provides the sedimentation coefficient (s) and calculated R values which were obtained by AUC for pd-FIX in the absence and presence of physiologic levels of Ca^{2+} and Mg^{2+}. We observed an $S_{20,w}$ of 3.72 ± 0.006 Svedburgs (n=3) by AUC in 10 mM EDTA at 0.3 mg pd-FIX/ml and this translates to an estimated R= 4.35 nm ± 0.006. This contrast previous AUC studies which showed an increase in FIX size due to aggregation [16]. These studies reported $S_{20,w}$ values were 4.17 Svedburgs for pd-FIX measured in the presence of 2 mM EDTA and also for 2.5 mM Ca^{2+} [16].

Since the presence of Ca^{2+} exerted a predominant effect on compactionas observed by HPSEC, we used the AUC observations obtained for 1.1 mm Ca^{2+} with or without Mg^{2+} as a statistical group for estimating its impact of the presence of Ca^{2+} on $S_{20,w}$: we obtained a value $S_{20,w}$ = 3.84 ± 0.014 Svedburgs (n=2) corresponding to R= 4.22 nm ± 0.014. In summary, the sedimentation behavior obtained by AUC supports a stark compaction effect by Ca^{2+} both observed by HPSEC and predicted by molecular modeling.

3.8. Estimation of the amount of compaction observed by HPSEC

We used the values of R obtained by AUC for X^{2+} free pd-FIX and in the presence of 1.1 mm Ca^{2+} to estimate column parameters needed to predict the change in R from all other HPSEC data. Fig. 8 shows a strong interpolative consistency for the R vs. Ca^{2+} concentration behavior using HPSEC values in the range of 0 to 1.1 mM Ca^{2+}. These values were trend-wise consistent with the remaining experimental values obtained by AUC not used to calibrate column parameters. At a physiologic level of Ca^{2+} at about which half maximal filling of Ca^{2+} specific sites occurs in the Gla domain, an overall decrease in R of 2.7% occurred relative to the X^{2+} free pd-FIX. An asymptotic decrease in R of about 5.6% was observed by HPSEC resulting from the complete filling of X^{2+} sites at supraphysiologic Ca^{2+} levels. The change in the R_g predicted by our modeling was similar at about 5%. In summary, we have shown that the holoprotein compaction phenomena due to both Mg^{2+} and Ca^{2+} can be quantitatively measured by HPSEC. Furthermore, the sensitivity of this measurement provides new insight into the cooperative nature of the folding phenomena between Gla and EGF1 domains not provided by previous studies using crystallography, circular dichroism and light scattering [14,52-55].

3.10. Scope and Limitations of Determining Compaction with HPSEC and AUC

We have demonstrated the use of HPSEC calibrated by AUC for determining the X^{2+} dependent compaction of VKD proteins. HPSEC is a greatly more facile technique than AUC for obtaining replicate analyses needed for statistical comparisons of data sets under different conditions. While a significant disadvantage is that at least 25 μg of highly purified material must be used to study the compaction with HPSEC, this material is fully recoverable. Using these methods, we have demonstrated that HPSEC is capable of detecting the changes in the radius of hydration on the scale of ~0.01 nm. The gradual filling

of X^{2+} sites in different domains of the VKD holoprotein can be detected on this scale due to this sensitivity. Within a purified mixture of rFIX, we showed that HPSEC is grossly capable of distinguishing between different levels of -carboxylated species due to differences in compaction. This then enables HPSEC to be used for the fractionation of subpopulations of VKD proteins from within the mixture.

Acknowledgements

We are grateful to Dr. Kevin Van Cott for performing all mass spectrometry described in this paper. The research was supported by National Institute of Health, National Heart, Lung and Blood Institute (R01 JL078944).

References

1. Furie B, Furie BC. Cell. 1988; 53:505. [PubMed: 3286010]
2. Davie EW, Fujikawa K, Kisiel W. Biochemistry. 1991; 30:10363. [PubMed: 1931959]
3. Vadivel, K.; Schmidt, AE.; Marder, VJ.; Krishnaswamy, S.; Bajaj, SP. Hemostasis and Thrombosis. Marder, VJ.; Aird, WC.; Bennett, HS.; Schulman, S.; White, GC., II, editors. Lippincott Williams and Willkins; Philadelphia, PA: 2013.
4. Soriano-Garcia M, Padmanabhan K, De Vos A, Tulinsky A. Biochemistry. 1992; 31:2554. [PubMed: 1547238]
5. Freedman SJ, Furie BC, Furie B, Baleja JD. Biochemistry. 1995; 34:12126. [PubMed: 7547952]
6. Mizuno H, Fujimoto Z, Atoda H, Morita T. Proceedings of the National Academy of Sciences. 2001; 98:7230.
7. Shikamoto Y, Morita T, Fujimoto Z, Mizuno H. Journal of Biological Chemistry. 2003; 278:24090. [PubMed: 12695512]
8. Freedman SJ, Furie BC, Furie B, Baleja JD. J Biol Chem. 1995; 270:7980. [PubMed: 7713897]
9. Huang M, Rigby AC, Morelli X, Grant MA, Huang G, Furie B, Seaton B, Furie BC. Nature Structural & Molecular Biology. 2003; 10:751.
10. Lewis RM, Furie BC, Furie B. Biochemistry. 1983; 22:948. [PubMed: 6838834]
11. Wakabayashi K, Sakata Y, Aoki N. Journal of Biological Chemistry. 1986; 261:11097. [PubMed: 3525561]
12. Orthner C, Madurawe RD, Velander WH, Drohan WN, Battey F, Strickland D. Journal of Biological Chemistry. 1989; 264:18781. [PubMed: 2478552]
13. Huang M, Furie BC, Furie B. J Biol Chem. 2004; 279:14338. [PubMed: 14722079]
14. Bajaj S. Journal of Biological Chemistry. 1982; 257:4127. [PubMed: 6978337]
15. de Courcy B, Pedersen L, Parisel O, Gresh N, Silvi B, Pilmé J, Piquemal J-P. Journal of chemical theory and computation. 2010; 6:1048. [PubMed: 20419068]
16. Amphlett GW, Kisiel W, Castellino FJ. Arch Biochem Biophys. 1981; 208:576. [PubMed: 6973319]
17. Li L, Darden TA, Freedman SJ, Furie BC, Furie B, Baleja JD, Smith H, Hiskey RG, Pedersen LG. Biochemistry. 1997; 36:2132. [PubMed: 9047312]
18. Wolberg AS, Li L, Cheung WF, Hamaguchi N, Pedersen LG, Stafford DW. Biochemistry. 1996; 35:10321. [PubMed: 8756687]
19. Gillis S, Furie BC, Furie B, Patel H, Huberty MC, Switzer M, Barry Foster W, Scoble HA, Bond MD. Protein science. 1997; 6:185. [PubMed: 9007991]
20. Messer A, Velander W, Bajaj S. Journal of Thrombosis and Haemostasis. 2009; 7:2151. [PubMed: 19817987]
21. Vo HC, Britz-Mckibbin P, Chen DD, MacGillivray RT. FEBS letters. 1999; 445:256. [PubMed: 10094467]
22. Degener A, Belew M, Velander WH. Journal of Chromatography A. 1998; 799:125. [PubMed: 9550105]

23. Straight DL, Sherrill G, Noyes C, Trapp H, Wright S, Roberts H, Hiskey R, Griffith M. Journal of Biological Chemistry. 1985; 260:2890. [PubMed: 3871774]
24. Van Cott KE, Butler SP, Russell CG, Subramanian A, Lubon H, Gwazdauskas F, Knight J, Drohan WN, Velander WH. Genetic analysis: biomolecular engineering. 1999; 15:155. [PubMed: 10596756]
25. Lindsay M, Gil G-C, Cadiz A, Velander WH, Zhang C, Van Cott KE. Journal of Chromatography A. 2004; 1026:149. [PubMed: 14763741]
26. Nichols T, Franck H, Franck C, De Friess N, Raymer R, Merricks E. Journal of Thrombosis and Haemostasis. 2012; 10:474. [PubMed: 22482117]
27. Nolte M, Nichols T, Mueller-Cohrs J, Merricks E, Pragst I, Zollner S, Dickneite G. Journal of Thrombosis and Haemostasis. 2012; 10:1591. [PubMed: 22726310]
28. Stafford WF 3rd. Anal Biochem. 1992; 203:295. [PubMed: 1416025]
29. E.J.a.E. Cohn, JT. Proteins, Amino Acids and Peptides as Ions and Dipolar Ions. Edsall, E.J.C.a.J.T., editor. Reinhold Publishing Corporation; New York: 1943. p. 370
30. Durschschlag, H. Thermodynamic Data for Biochemistry and Biotechnology. Hinz, HJ., editor. Springer-Verlag; Berlin: 1986. p. 45
31. Cole JL, Lary JW, Moody TP, Laue TM. Methods in cell biology. 2008; 84:143. [PubMed: 17964931]
32. Perera L, Darden TA, Pedersen LG. Thromb Haemost. 2001; 85:596. [PubMed: 11341491]
33. Eswar N, Webb B, Marti-Renom MA, Madhusudhan MS, Eramian D, Shen MY, Pieper U, Sali A. Curr Protoc Bioinformatics. 2006 Chapter 5 Unit 5 6.
34. Brooks BR, Bruccoleri RE, Olafson BD, States DJ, Swaminathan S, Karplus M. Journal of Computational Chemistry. 1983; 4:187.
35. Calcaterra J, Van Cott KE, Butler SP, Gil GC, Germano M, van Veen HA, Nelson K, Forsberg EJ, Carlson MA, Velander WH. Biomacromolecules. 2013; 14:169. [PubMed: 23215461]
36. Jagadeeswaran P, Sheehan JP. Blood Cells, Molecules, and Diseases. 1999; 25:239.
37. Bajaj SP, Schmidt AE, Agah S, Bajaj MS, Padmanabhan K. J Biol Chem. 2006; 281:24873. [PubMed: 16757484]
38. Vadivel K, Agah S, Messer AS, Cascio D, Bajaj MS, Krishnaswamy S, Esmon CT, Padmanabhan K, Bajaj SP. Journal of molecular biology. 2013
39. Handford PA, Baron M, Mayhew M, Willis A, Beesley T, Brownlee GG, Campbell ID. EMBO J. 1990; 9:475. [PubMed: 2406129]
40. Bajaj SP, Sabharwal AK, Gorka J, Birktoft JJ. Proc Natl Acad Sci U S A. 1992; 89:152. [PubMed: 1729682]
41. Zögg T, Brandstetter H. Structure. 2009; 17:1669. [PubMed: 20004170]
42. Samis JA, Ramsey GD, Walker JB, Nesheim ME, Giles AR. Blood. 2000; 95:943. [PubMed: 10648407]
43. Rao Z, Handford P, Mayhew M, Knott V, Brownlee GG, Stuart DZ. Cell. 1995; 82:131. [PubMed: 7606779]
44. Sekiya F, Yamashita T, Atoda H, Komiyama Y, Morita T. Journal of Biological Chemistry. 1995; 270:14325. [PubMed: 7782291]
45. Deerfield D, Olson D, Berkowitz P, Byrd P, Koehler K, Pedersen L, Hiskey R. Journal of Biological Chemistry. 1987; 262:4017. [PubMed: 3558405]
46. Banner DW, D'Arcy A, Chene C, Winkler FK, Guha A, Konigsberg WH, Nemerson Y, Kirchhofer D. Nature. 1996; 380:41. [PubMed: 8598903]
47. Gillis S, Furie BC, Furie B, Patel H, Huberty MC, Switzer M, Foster WB, Scoble HA, Bond MD. Protein Sci. 1997; 6:185. [PubMed: 9007991]
48. Kaufman RJ, Wasley LC, Furie BC, Furie B, Shoemaker CB. J Biol Chem. 1986; 261:9622. [PubMed: 3733688]
49. Laurent TC, Killander J. Journal of Chromatography A. 1964; 14:317.
50. Ackers G. Journal of Biological Chemistry. 1967; 242:3237.

51. Fish WW, Reynolds JA, Tanford C. Journal of Biological Chemistry. 1970; 245:5166. [PubMed: 5528243]
52. Agah S, Bajaj SP. J Thromb Haemost. 2009; 7:1426. [PubMed: 19500239]
53. Nelsestuen GL, Resnick RM, Wei GJ, Pletcher CH, Bloomfield VA. Biochemistry. 1981; 20:351. [PubMed: 7470485]
54. Amphlett GW, Byrne R, Castellino FJ. Journal of Biological Chemistry. 1978; 253:6774. [PubMed: 690125]
55. Amphlett GW, Byrne R, Castellino FJ. Journal of Biological Chemistry. 1979; 254:6333. [PubMed: 447718]

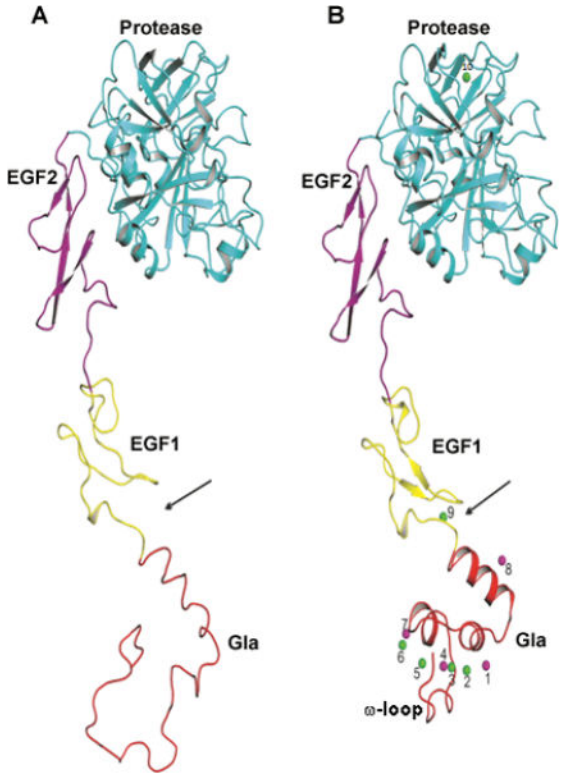

Fig. 1.

Modeled structures of intact FIX without (A) and with (B) X^{2+} ions predicted from the crystallographic data. The Gla, EGF1-like, EGF2-like and the protease domain in FIX are colored red, yellow, purple and cyan, respectively. FIX contains 10 Ca^{2+}/Mg^{2+} binding sites, which are numbered 1 through 10; eight of these are in the Gla domain (number 1-8), one in the EGF1-like domain (number 9) and one in the protease domain (number 10). The Ca^{2+}-specific sites are shown as green spheres, whereas the sites 1, 4, 7 and 8 could be occupied by either Ca^{2+} or Mg^{2+} are shown as magenta spheres. As a result of X^{2+} binding, a major structural change occurs in the Gla domain and a minor change in the EGF1-like domain of FIX. The properly formed ω-loop is clearly visible and positioned below metal sites 3, 4 and 5.

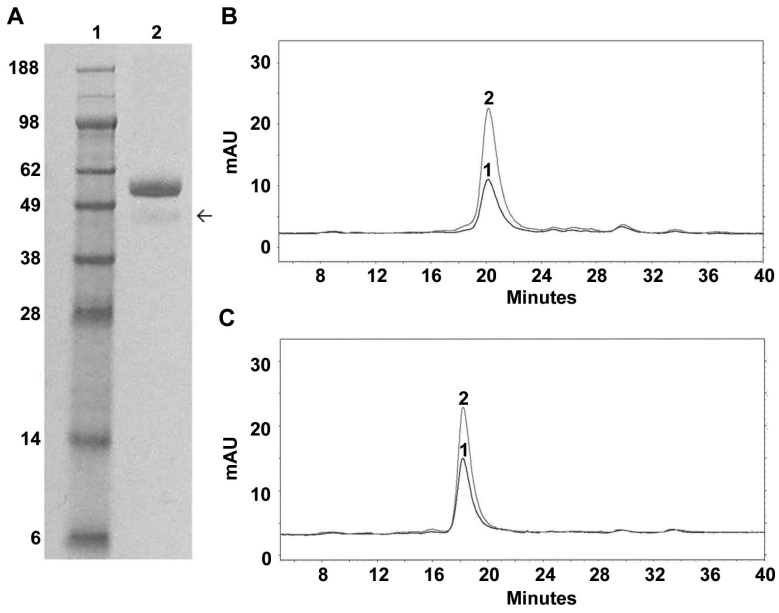

Fig. 2.

Homogeneity and extent of aggregation of starting samples of purified FIX. SDS-PAGE and HPSEC as a function of the injection amount was studied: A) Non-reducing SDS-PAGE of purified FIX: Lane 1. Molecular weight markers; Lane 2. FIX (2 μg). Arrow indicates proteolyzed pd-FIX. B) HPSEC chromatographic profiles of FIX at 25 μg (curve 1) and at 50 μg injected (curve 2) at physiologic 1.1 mM Ca^{2+} and C) HPSEC chromatographic profiles of FIX at 25 μg (curve 1) and at 50 μg injected (curve 2) at physiologic 0.6 mM Mg^{2+}.

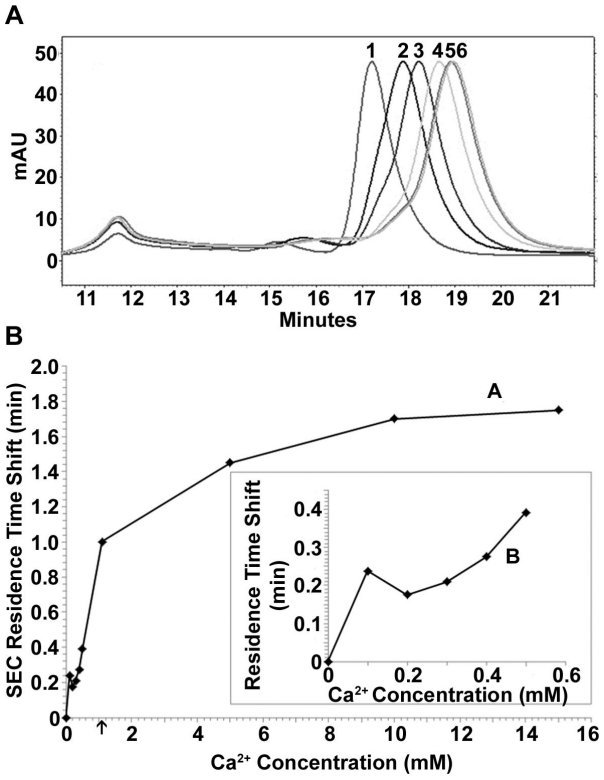

Fig. 3.

HPSEC residence time behavior of FIX in the presence of $CaCl_2$ only. In each case, amount of FIX injected was 100 μg. A) Curve 1: no X^{2+}, Curve 2: 0.5 mM $CaCl_2$, Curve 3: 1.1 mM $CaCl_2$, Curve 4: 5 mM $CaCl_2$, Curve 5: 10 mM $CaCl_2$, Curve 6: 15 mM $CaCl_2$. B) Net residence time shift in the HPSEC residence time by FIX with change in $CaCl_2$ concentration in the range from 0 - 15 mM; *inset*, magnified view of residence time shift induced in the range from 0 – 0.5 mM $CaCl_2$. Each data point condition was performed in triplicate with a standard deviation <0.016 minutes. Arrow indicates physiological levels of $CaCl_2$.

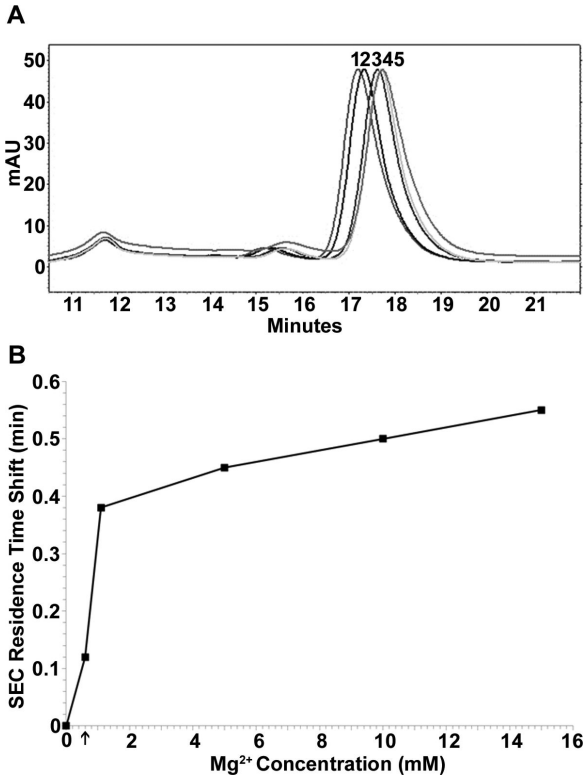

Fig. 4.

HPSEC residence time behavior of FIX in the presence of $MgCl_2$ only. In each case, amount of FIX injected was 100 μg. A) Curve 1: no X^{2+}, Curve 2: 0.6 mM $MgCl_2$, Curve 3: 5 mM $MgCl_2$, Curve 4: 10 mM $MgCl_2$, Curve 5: 15 mM $MgCl_2$. B) Net residence time shift in the HPSEC residence time by FIX with change in $MgCl_2$ concentration in the range from 0 - 15 mM. Each data point condition was performed in triplicate with a standard deviation <0.016 minutes. Arrow indicates physiological levels of $MgCl_2$.

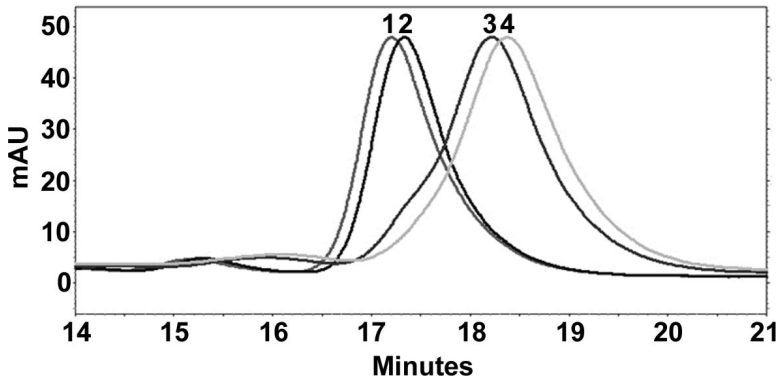

Fig. 5.

HPSEC residence time behavior of FIX in the presence of physiologic levels of both $CaCl_2$ and $MgCl_2$: Curve 1: no X^{2+}, Curve 2: 0.6 mM $MgCl_2$, Curve 3: 1.1 mM $CaCl_2$, Curve 4: 1.1 mM $CaCl_2$ & 0.6 mM $MgCl_2$. Each data point condition was performed in triplicates with a standard deviation <0.016. Arrows indicate physiological levels of $MgCl_2$ or $CaCl_2$.

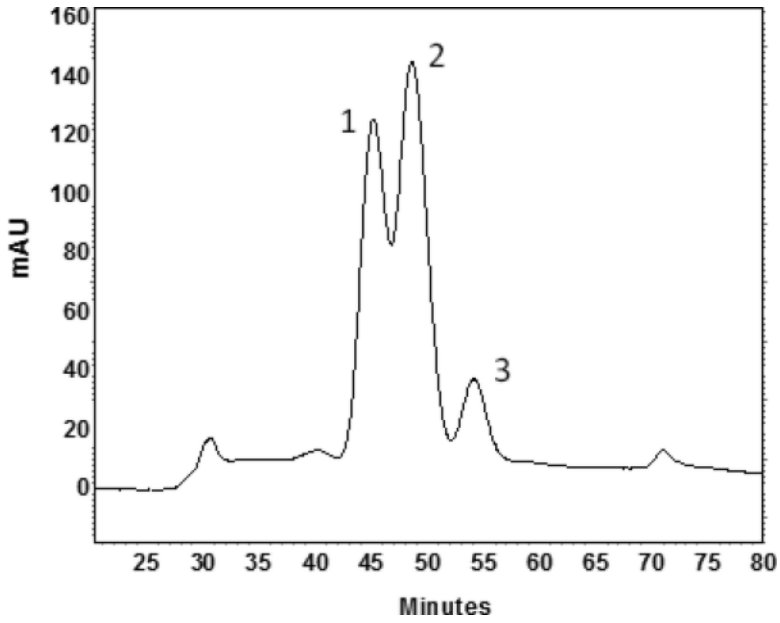

Fig. 6.

HPSEC chromatogram of the fractionation of purified r-FIX populations. Table 1 presents characterization of Peak 1 and Peak 2. Peak 1) low Gla, inactive r-FIX; Peak 2) high Gla, active FIX; Peak 3) FIXa.

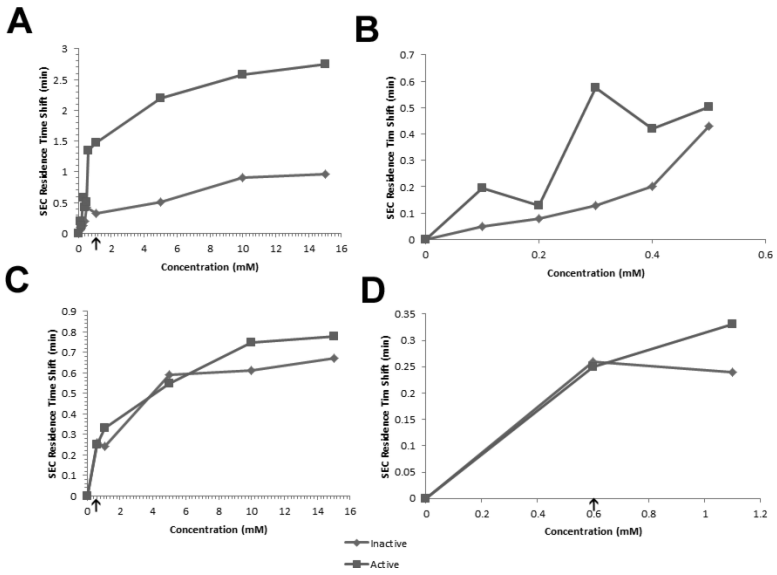

Fig. 7.

HPSEC net residence time shift of r-FIX in the presence of 0-15 mM $MgCl_2$ and $CaCl_2$. In each case, amount of r-FIX injected was 100 μg. A) 0-15 mM $CaCl_2$ B) 0-0.5 mM $CaCl_2$ C) 0-15 mM $MgCl_2$ D) 0-1.1 mM $MgCl_2$. Each data point condition was performed in triplicate with a standard deviation <0.016 minutes. Arrows indicate physiological levels of $MgCl_2$ or $CaCl_2$.

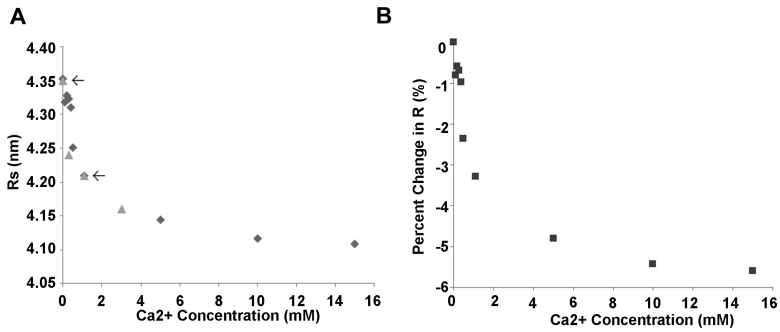

Fig. 8.

Estimated $CaCl_2$-dependent change in Stokes radius of FIX as measured by HPSEC. R values by HPSEC made by correlation method of Laurent and Killander [33], Acker [34], and Fish and Reynolds et al. [35]. A) ◆ HPSEC Value; ▲ AUC Value B) ■ Percent change in R estimated by HPSEC (%). Arrows indicate AUC values used to determine coefficient of the HPSEC correlation.

Table 1

Total Gla content and activity of purified r-FIX populations fractionated by HPSEC.

Sample	Total Gla Content	% Gla	Activity (Units/mg)	% FIXa
pd-FIX	12 Gla	100	200	0
Peak 1	10 Gla	>30	3	0
	6-9 Gla	<70		
Peak 2	10-12 Gla	>80	249	0
	8-9 Gla	<20		

Table 2

Sedimentation coefficients and estimated Stokes radii from analytical centrifugation of FIX. The sedimentation coefficient S is given for FIX centrifuged in the presence of EDTA, Ca^{2+} and/or Mg^{2+}.

Solvent[1]	$S_{20,w}$ (Svedberg)	Stokes Radius (nm)
10 mM EDTA	3.71	4.36[a]
10 mM EDTA	3.72	4.35[a]
10 mM EDTA	3.72	4.35[a]
0.6 mM MgCl2	3.82	4.24
0.6 mM MgCl2 + 1.1 mM CaCl2	3.83	4.23
0.3 mM CaCl2	3.82	4.24
1.1 mM CaCl2	3.85	4.21[a]
3.0 mM CaCl2	3.89	4.16

[a] Used to determine coefficient of the SEC correlation by methods developed in Laurent and Killander (1964).

[1] The buffer contained 50 mM Tris, 0.15 M NaCl, pH 7.5 and either EDTA or X^{2+} as indicated